Experimental Analysis of UAVs Operations on Military Frigates

Rafael Bardera Mora
Juan Carlos Matías García
Estela Barroso Barderas
Javier Muñoz Campillejo

Experimental Aerodynamics
Instituto Nacional de Técnica Aeroespacial (INTA)
Torrejón de Ardoz, Madrid
SPAIN

barderar@inta.es

ABSTRACT

Military operations combining frigates and aircraft operations can increase enormously the possibilities and the chances of mission success. Traditionally, these kinds of operations on frigates are conducted with helicopters. Nevertheless, there is a growing interest in using Unmanned Aerial Vehicles (UAVs) in military operations from frigates. For example, for helping in maritime operations, rescue, or border surveillance. The UAVs have the great advantage of a lower cost of acquisition and operation compared to helicopters and reduce the risk of human losses by not needing a pilot on-board. However, as in the case of helicopters, when they operate above the frigate flight deck, the UAVs must face a turbulent flow with high-velocity gradients, generated by the non-aerodynamic surfaces of the military vessels. The goal of the present work is to characterize the aerodynamic problems of the flow where UAVs have to operate around the frigate. For this purpose, velocity measurements in wind tunnel are taken on the wake of a three-dimensional descending step that represents the rear part of a frigate at 1:22 scale, where the flight deck is usually located. Particle Image Velocimetry (PIV) is used to extract velocity maps of the detached flow above the flight deck, and sonic anemometry is employed to obtain averaged velocities, turbulence levels, and frequency spectra at five different points of the wake, within a control volume that a typical UAV can occupy.

1.0 INTRODUCTION

Aircraft and military frigates combined operations are very effective. They contribute to higher mission effectiveness. Helicopters have been traditionally used in combination with military frigates. However, in recent years and with the high development of Unmanned Aerial Vehicles (UAV), their use in frigates is becoming popular. They have great advantages such as lower acquisition and operating costs and lower risk of losses produced by an accident. As an example, in October 2020, the Spanish Navy conducted the first flight test of an RPAS over the frigate Reina Sofia (Figure 1-1). Another example is the Alpha 900, an unmanned helicopter that the Greek navy has purchased to operate in combination with frigates. Even so, UAV operations on frigates can be complex and high-risk operations. The ship movement and the turbulent flow generated by the non-aerodynamic shapes of the frigate make it necessary to know in-depth the characteristics of the flow above the flight deck. This flight deck is usually located behind the superstructure. In particular, the study of velocities, turbulence and flow frequencies in this part of the ship is essential to know and predict possible interferences with the UAV operation. The determination of the flow field is also crucial to locate the shear layer and the recirculation bubble generated by the ship. Both can seriously affect the safety of the UAV maneuvers near the frigate. There are several examples of numerical studies [1-4], wind tunnel tests [5-8], and helicopter operations studies [9-15] on frigates to characterize the flow around them. They are interesting to know the main characteristics of the flow above the flight deck and help increase the safety of these operations.

Figure 1-1: Flight tests of Scan Eagle above "Reina Sofía" spanish Frigate.

As the flight deck is usually placed at the aft and behind the superstructure of the frigate, it can be modeled as a three-dimensional descending step. In this work, an experimental analysis of the flow behind a modified descending step, which represents the aft-deck of a frigate, is conducted by means of ultrasonic anemometry. This kind of measurements extracts mean velocities inside a flow volume. As can be seen in figure 1-2, using a proper scale of the frigate model (1:22), the measurement volume of 250 mm can represent the size of a typical UAV that operates on a military frigate (5 m). The paper is divided into three main sections: experimental set up where the wind tunnel, frigate model, and velocity measurement techniques are explained, the results section where the Particle Image Velocimetry and ultrasonic anemometer measurements are presented and a summary of the conclusions extracted from the study.

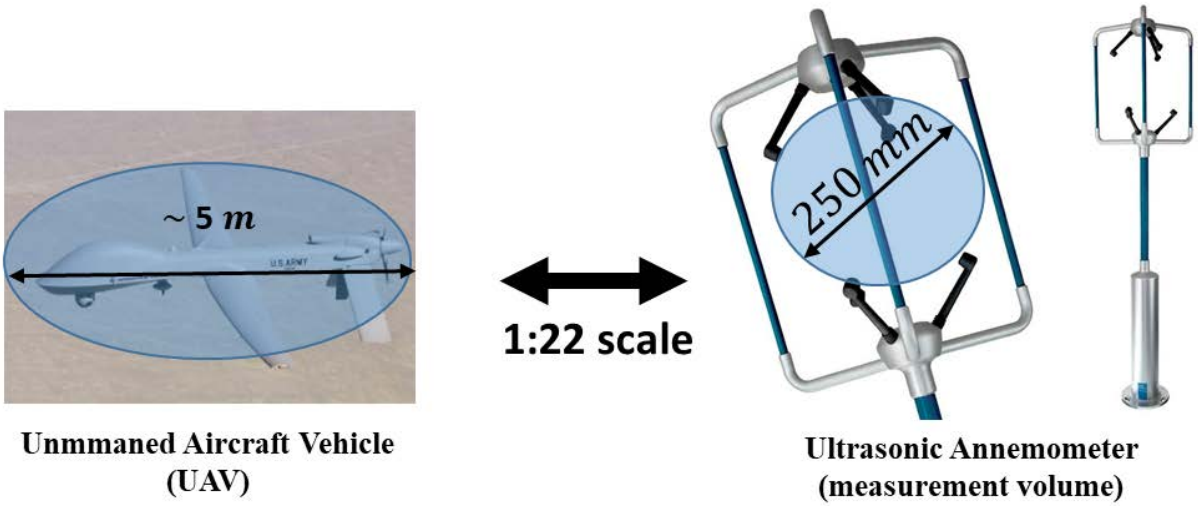

Figure 1-2: Measurement volume of an ultrasonic anemometer compared to a 1:22 scaled UAV.

2.0 EXPERIMENTAL SET-UP

In this section the experimental facilities used for testing, the frigate scaled model and velocity measurement techniques will be described.

2.1 Low-speed wind tunnel

The low-speed wind tunnel T1 of the National Institute for Aerospace Technology (INTA) is located at Torrejón de Ardoz (Spain), figure 2-4 (a). It is a closed-circuit wind tunnel with an open and elliptical test section of 2 m × 3 m and 3.5 m of length. Inside the tests section, there is a moving platform that represents the sea surface where the scaled frigate models can be placed for testing. The maximum velocity of the air that can be reached during the tests is 60 m/s. The engine has a maximum power of 450 kW at 420 V. The wind tunnel allows tests with low turbulence intensity (≤ 0.5 %) and Reynolds number up to 4 million/m.

2.2 Frigate aft-deck scaled model

The goal of the study is to characterize the flow above the flight deck of the frigate. This deck is placed right behind the superstructure. As can be seen in the Simple Frigate Shape model represented in figure 2-1, the geometry of this part of the frigate forms a descending step geometry. In order to increase the Reynolds number during the tests, the size of the model is maximized and only the descending step of the frigate is represented in figure 2-1 (right). The maximum size of the model is limited by the non-blockage condition of the wind tunnel. In this way, the front section of the model at 1:22 scale (0.36 m2) is lower than the 10 % of the wind tunnel test section.

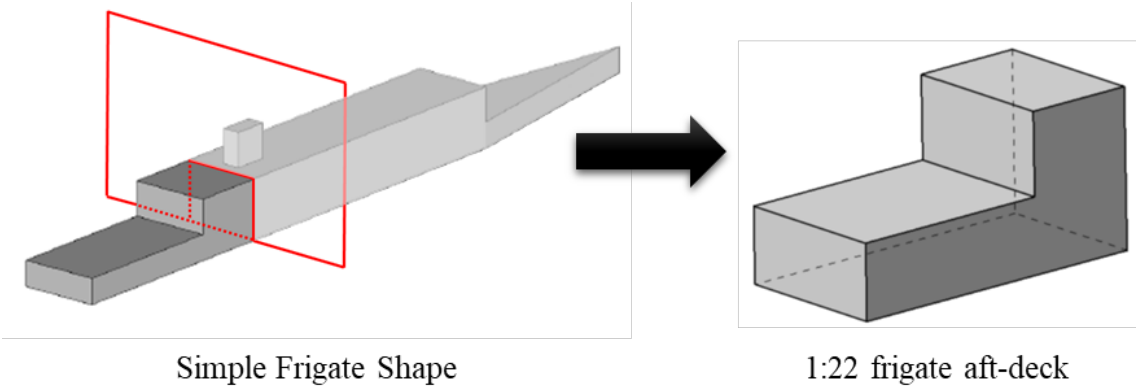

Figure 2-1: Simple Frigate Shape model and 1:22 scaled model of the aft-deck of the frigate.

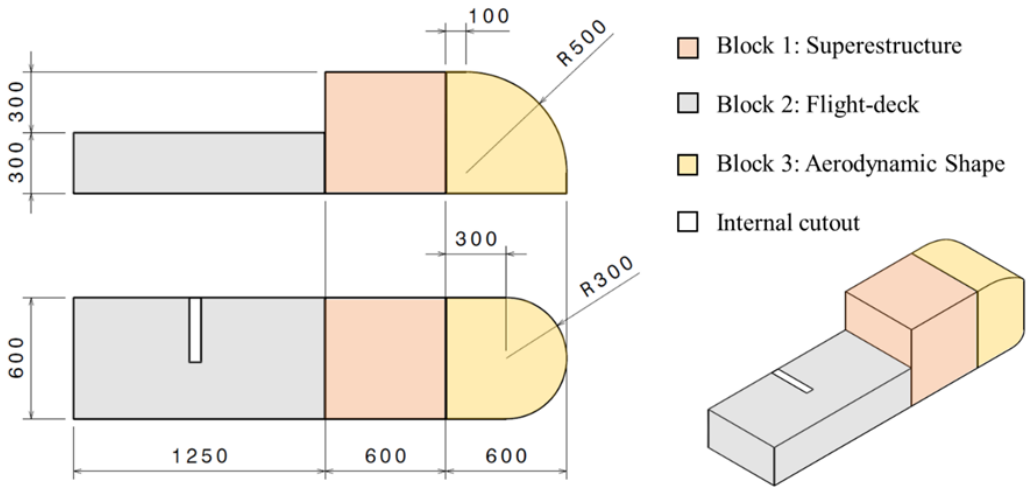

Figure 2-2: Blocks of the 1:22 scaled aft-deck for testing.

In figure 2-2 the three blocks that compose the model tested at the wind tunnel are shown. The first one is a wooden box with a size of 60 × 60 × 60 cm3 that represents the rear part of the frigate superstructure. The second block corresponds to the frigate aft-deck and its dimensions are 1250 cm in length, 60 cm of wide, and 30 cm in height. It has been manufactured of expanded polystyrene, which is a suitable material for hot wire cutting. This allows performing an internal cutout to hide the ultrasonic anemometer in different positions during the tests, avoiding aerodynamic interference. In each position, the remaining holes that the anemometer does not occupy are covered with the same material, avoiding flow alterations. In addition, the blocks are painted with black lines to avoid laser reflections during PIV tests.

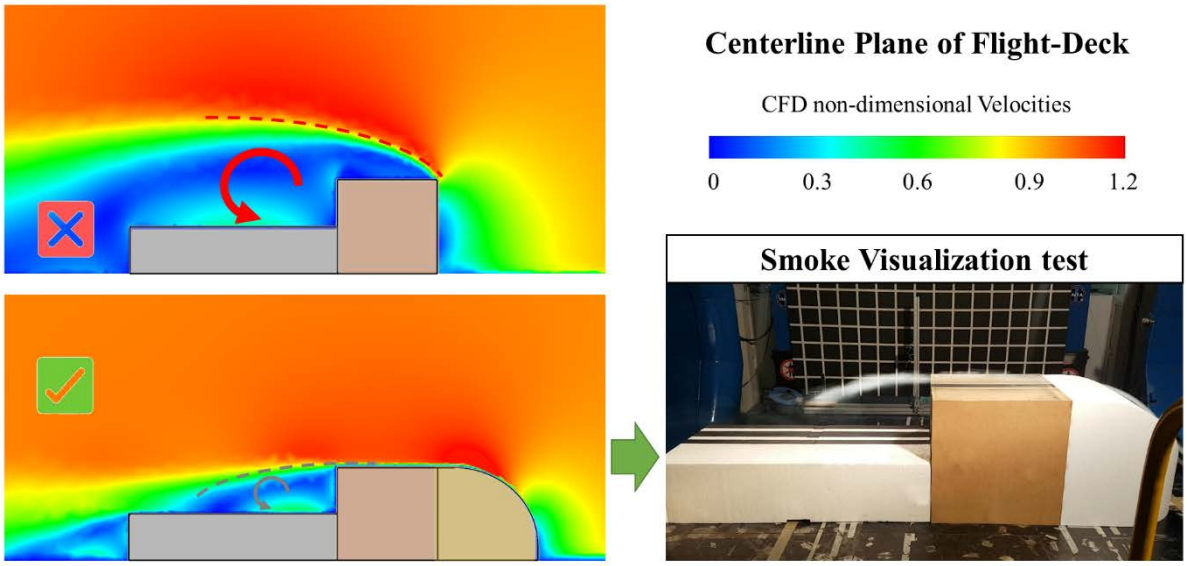

Figure 2-3: Aerodynamic effect of the front block.

Due to length restrictions at the wind tunnel, a 1:22 full-scaled frigate does not fit at the test section. Then, a third block is placed upstream of the previous ones to achieve the same aerodynamics on the deck to the full frigate. In a complete frigate, due to the length of the superstructure and before reaching the flight deck, the flow is attached on the top. Then, the third block, which is also manufactured with expanded polystyrene and hot wire cut, has an aerodynamic shape to avoid an abrupt detachment of the flow, in order to reproduce adequately the boundary condition, figure 2-2. To check the proper working of the third block, a CFD simulation and a smoke visualization test were performed with the aerodynamic block. The results shown in figure 2-3 demonstrate that the flow detachment starts behind the superstructure, as in a full frigate.

2.3 Particle Image Velocimetry (PIV)

Particle Image Velocimetry (PIV) is an advanced velocity measurement technique that captures the position of small particles seeded in the flow in order to measure their displacement and velocity, which corresponds to the velocity of the flow [16-19].

The PIV needs different components to work (figure 2-4 (b)). A particles seeding system, composed of Laskin atomizers, generates atomized particles of olive oil with a size of 1 μm. Two pulsed neodymium lasers are used to illuminate the flow region to study. A recording system composed of a digital camera (2048 × 2048 pixels) with the proper lens installed. A synchronizer to trigger the laser pulses and the camera at the proper time. Finally, the whole system is controlled by a computer with the software “Insight 3G”.

The specific experimental set-up used for the tests has a Field of View (FOV) of 50 cm, a Fast Fourier Transform (FFT) for the correlation process that gets the velocity vectors on each pair of images obtained, a size of analysis window of 32 × 32 pixels, and a delay time between laser pulses of 25 μs.

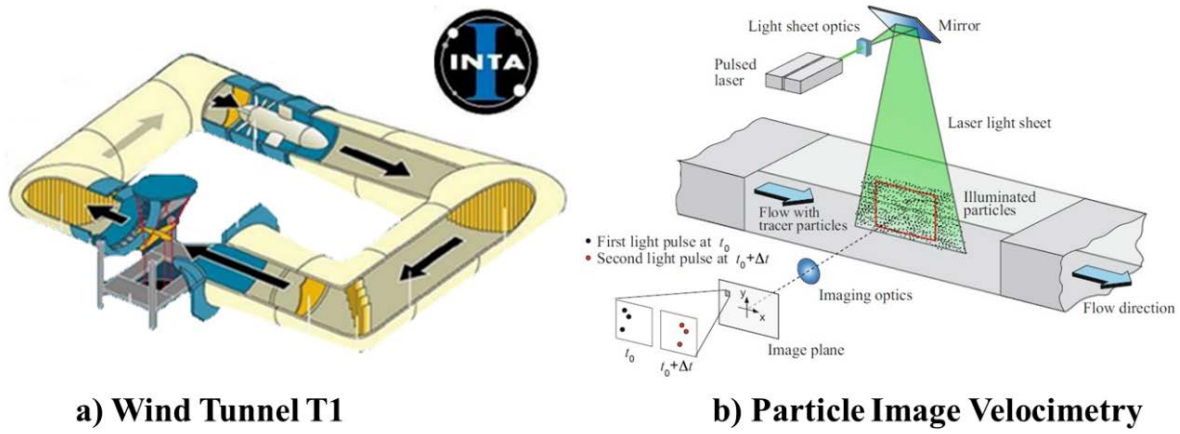

Figure 2-4: a) Wind tunnel T1 at INTA b) Particle Image Velocimetry (PIV) system.

2.4 Ultrasonic anemometry

Ultrasonic anemometry is a velocity measurement technique based on the use of ultrasonic waves to determine the velocity of a flow. The ultrasonic anemometer that measures three velocity components consists of three pairs of transducers. An ultrasonic pulse is emitted from the upper transducer to the opposite transducer. Another pulse is emitted in the opposite direction. The time that the pulses last to travel the distance between the transducers is measured (t_1 and t_2). As the velocity of sound (c), distance (L), and times are known, the velocity of the flow can be obtained using the following expressions [20],

$$t_1 = \frac{L}{c+V} \qquad t_2 = \frac{L}{c+V} \tag{1}$$

$$V = \frac{L}{2}\left(\frac{1}{t_1} - \frac{1}{t_2}\right) \tag{2}$$

This operation is performed for the three pairs of transducers so that the velocity vector from three components of velocity, in Cartesian or polar coordinates, is determined. In addition, it is important to note that the velocity measurement obtained is independent of factors such as temperature, pressure, or humidity.

Finally, during the tests, the ultrasonic anemometer used is a WindMaster 1590-PK-020/W and is connected to a power source and to a computer with the control software supplied by the manufacturer of the anemometer. The connection to the computer is via a standard RS-422 serial connector and a Serial to USB converter Moxa Uport 1650-8. The data sampling can be adjusted at 8 Hz, 20 Hz, or 32 Hz, which is the maximum recording frequency allowed by the anemometer used.

During the wind tunnel tests, the anemometer is placed in five different positions with respect to the scaled flight deck. These positions correspond to the positions where the UAV can be during the type “L” manoeuvres above the flight deck. The five measurements (points 1 to 5 in figure 2-5) are at 0 mm, 80 mm, 160 mm, 240 mm, and 300 mm from the flight deck centre and at 318 mm of height from the deck surface. This height is critical since it is inside the shear layer produced by the flow detachment on the superstructure. Therefore, it

could be a complex zone for the operation of UAVs, from the point of view of velocity gradients and turbulence intensity. In order to change the point of measurement, as the anemometer is installed in a fixed position, the scaled model is moved across the platform. At each position, data is taken for 1 minute at wind speeds of 10 and 15 m/s.

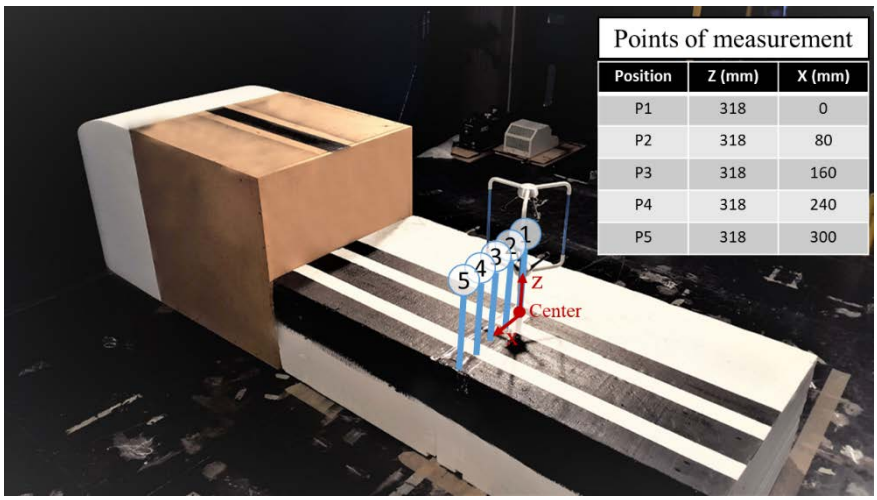

Figure 2-5: Positions of the ultrasonic anemometer during wind tunnel testing.

3.0 RESULTS

3.1 PIV Non-dimensional velocity maps

In this section, velocity maps obtained with PIV on the scaled flight deck are analyzed. The PIV tests allow determining the velocity field in three equidistant planes. One is placed at the symmetry axis (P1), another (P2) at 150 mm from P1, and the last one (P3) placed at 300 mm from the first.

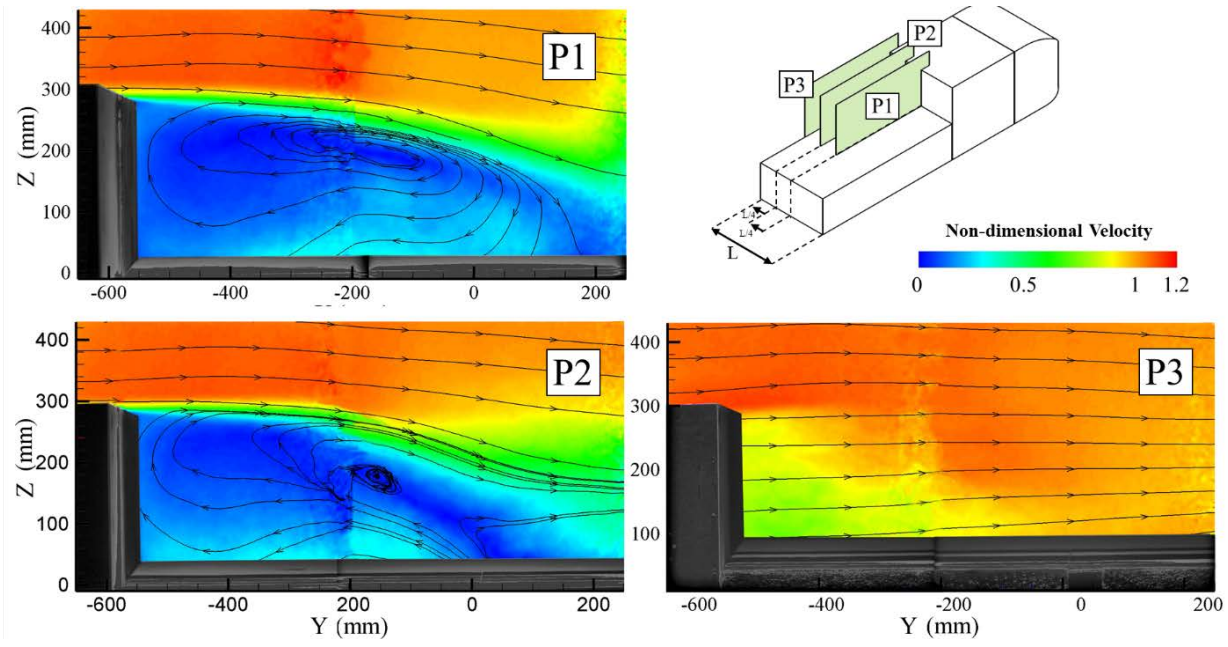

Figure 3-1: Positions of the ultrasonic anemometer during wind tunnel testing.

The results displayed in figure 3-1 show a recirculation bubble in the wake of the three-dimensional descending step that reaches the center of the flight deck. This way, it clearly interferes with UAV operations on frigates. The shear layer produced by the flow detachment is also visible. It divides a region with velocities close to 1 and another region with lower velocities (between 0.3 and 0.9 in non-dimensional terms). The velocity measurements with the anemometer are taken at this height, where the velocity values constantly change, causing a turbulent and dangerous flow for the operation of UAVs.

3.2 Ultrasonic anemometer: velocity measurements

In this section, a first amplitude analysis of the signal obtained at each anemometer position (figure 2-5) is carried out. The following tables 3-1 and 3-2 show the mean velocities and standard deviations for the three components of the velocity vector: U, V and W respectively, and for the two velocities tested in the wind tunnel: $U_\infty = 10$ and 15 m/s.

Table 3-1. Non-dimensional velocities, standard deviations and turbulence intensity for points P1 to P5, $U_\infty = 10$ m/s

Position	U	V	W	σ_U	σ_V	σ_W	TI
1	0.99	0.03	0.21	0.32	0.24	0.24	2.69
2	0.82	0.09	0.33	0.70	0.59	0.53	6.11
3	0.56	0.17	0.21	1.28	1.05	1.21	11.84
4	0.85	0.24	0.13	0.90	0.62	0.68	7.43
5	0.98	0.21	0.07	0.42	0.28	0.34	3.51

Table 3-2. Non-dimensional velocities, standard deviations and turbulence intensity for points P1to P5. $U_\infty = 15$ m/s

Position	U	V	W	σ_U	σ_V	σ_W	TI
1	0.69	0.03	0.29	0.12	0.09	0.09	15.52
2	0.70	0.11	0.30	0.13	0.09	0.08	15.13
3	0.57	0.17	0.22	0.12	0.09	0.10	15.73
4	0.82	0.22	0.13	0.09	0.05	0.06	10.03
5	0.95	0.20	0.07	0.04	0.03	0.03	5.27

The same non-dimensional velocity data (U/U_∞, V/U_∞ and W/U_∞) is presented in figure 3-2. The x-axis has the non-dimensional position (P1 to P5) with respect to the width of the scaled model (60 cm), taking the origin on the center of the flight deck. As can be determined with the data given, there must be vortex in the flow measured since the velocity along the main flow direction (U) suffers variations on each position and the other velocity components (V and W) are not negligible.

From the velocity measurements, the turbulence intensity (TI) is represented also for each point in figure 3-2, and has been obtained with the following expression,

$$TI\ (\%) = \frac{\sigma_V}{U_\infty} \cdot 100 \tag{3}$$

where $\sigma_V = \sqrt{\frac{1}{3}(\sigma_u^2 + \sigma_v^2 + \sigma_w^2)}$

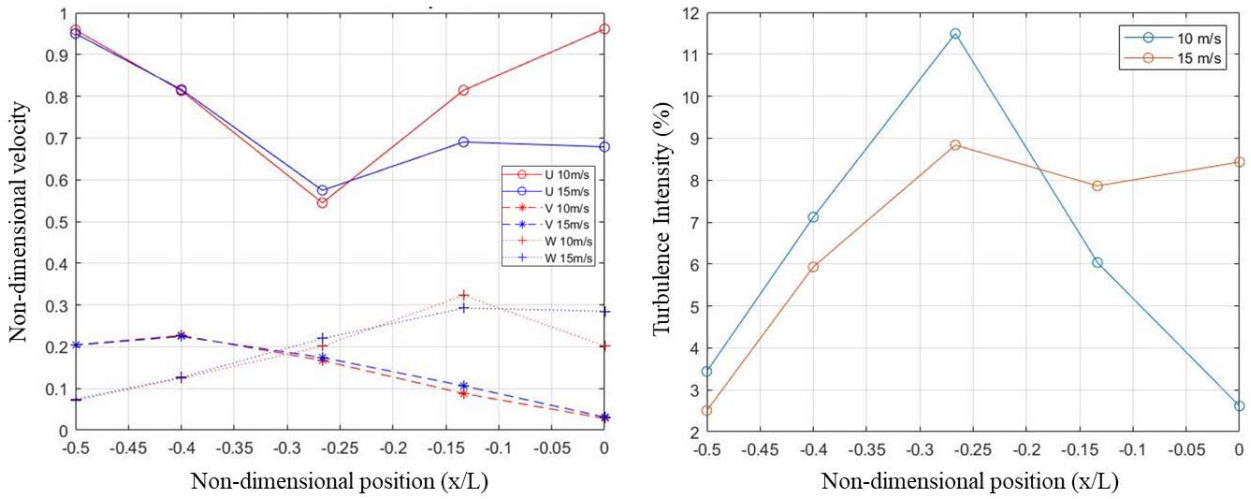

Figure 3-2: Positions of the ultrasonic anemometer during wind tunnel testing.

3.3 Ultrasonic anemometer: spectral analysis

The frequency analysis and the spectrum of the signal help in determining characteristic frequencies of the turbulent flow that could affect the UAV operation around the frigate. The spectral analysis allows the determination of vortex shedding frequencies. Then, the signals are spectrally analyzed to determine if the vortex frequencies that appear in the shear layer are in the frequency range between 0 and 16 Hz. Low-frequency vortex can affect the UAV operation and remoted pilot workload [21]. For this purpose, the spectra of the signals measured for each velocity component at the five positions studies are obtained. Specifically, the results of Power Spectral Density (PSD) for each velocity component and position is presented in figures 3-3 and 3-4.

PSD presented in figure 3-3 for $U_\infty = 15\ m/s$ has different aspects to highlight. The U velocity has peaks at positions P3 and P4 for frequencies between 2 and 4 Hz and between 13 and 16 Hz. In addition, position 3 also shows less intense peaks for frequencies in a range from 13 to 15 Hz. For the transversal velocity V, there are peaks for frequencies of 3 Hz, 12 Hz, 13 Hz and 14 Hz. Finally, the spectra of vertical velocity W, there is a noticeable peak at a frequency of 4 Hz. There are others frequency peaks between 10, 14 and 16 Hz, but they have lower intensity.

For $U_\infty = 10\ m/s$ cases presented in figure 3-4, PSD of components U and V do not present any relevant frequency peaks at any of the UAV positions. However, the component W has peaks at 1, 1.8, 2.5 Hz and 13 and 15 Hz for position 1 (P1) and at 5, 11, 13 and 14.5 Hz for position 3 (P3).

4.0 CONCLUSIONS

In this work, the flow inside the turbulent wake of a three-dimensional descending step of a rear part of a frigate has been experimentally analyzed. The goal has been characterizing the velocity and turbulence intensity at different points where a UAV can operate around a frigate. By means of the PIV measurement technique, non-dimensional velocity maps have been obtained. Using three different planes, the flow recirculation bubble that generates the superstructure flow detachment has been clearly visible. After the PIV measurements, an ultrasonic anemometer has been used to measure the three components and the standard

deviations of velocities inside a control volume given by the size of the anemometer measurement volume. Properly scaled, this volume represents the size of a UAV that can operate on a frigate.

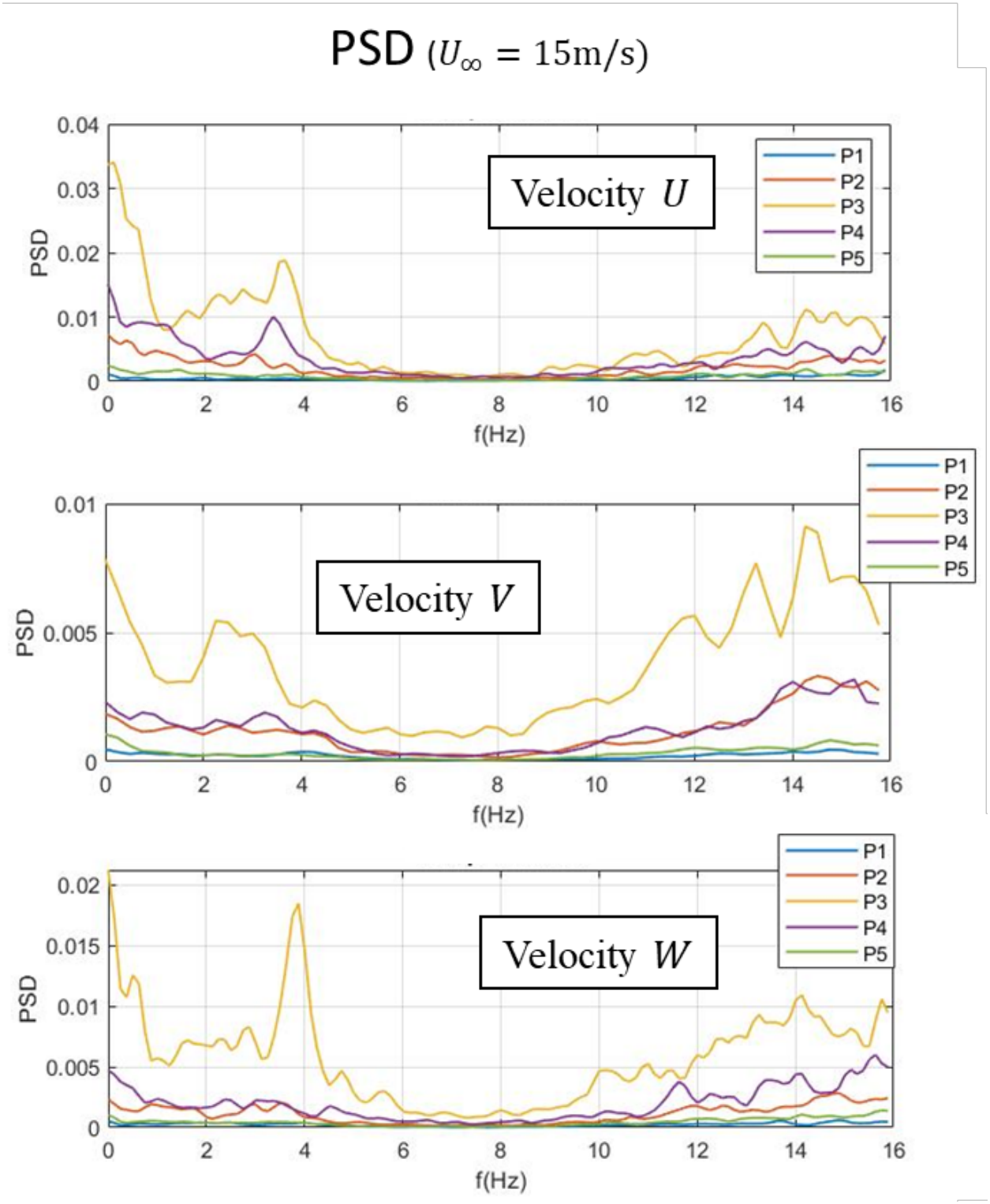

Figure 3-3: PSD spectra for P1 to P5; $U_\infty = 15\ m/s$

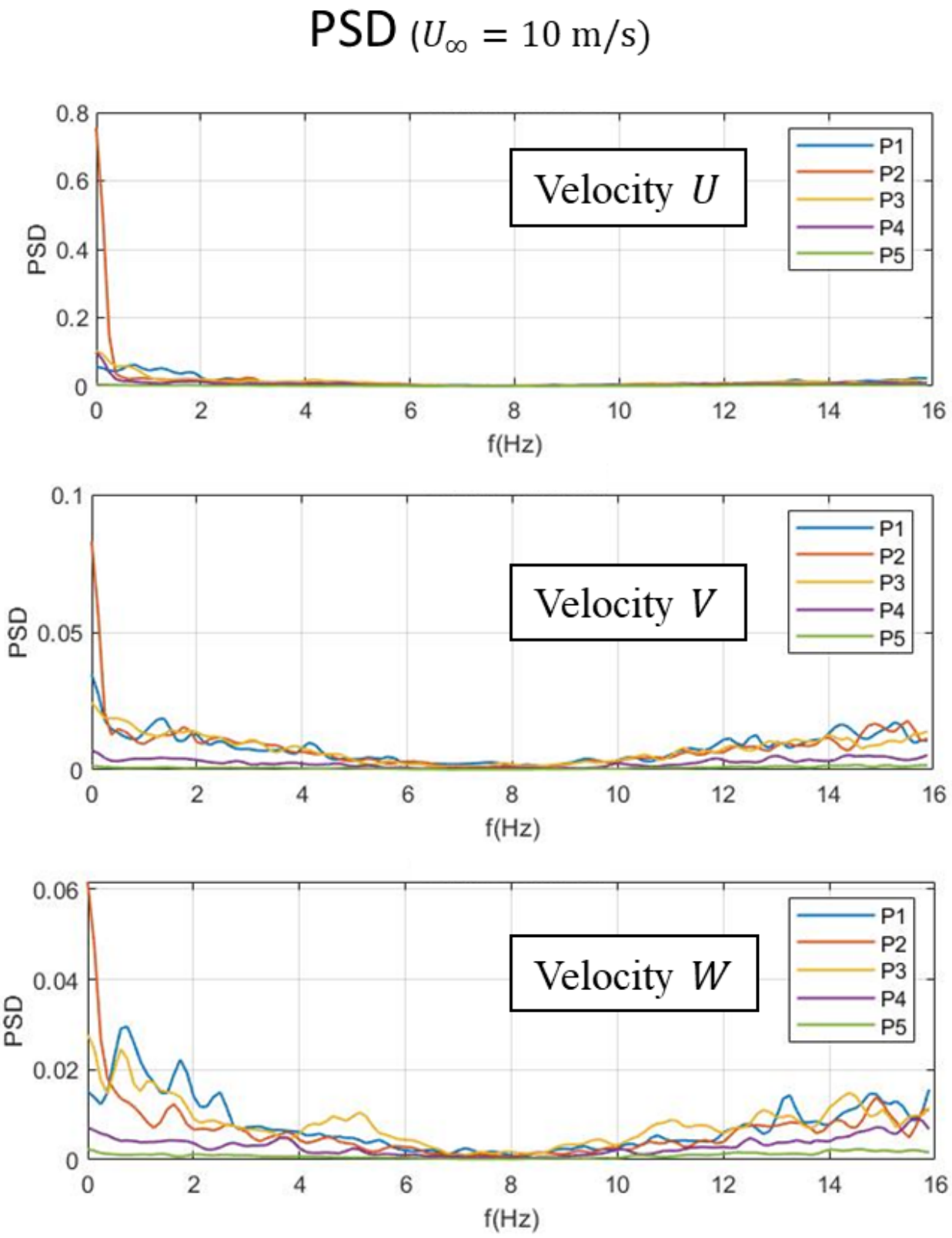

Figure 3-4: PSD spectra for P1 to P5; $U_\infty = 10\ m/s$

4.1 Next-steps

The results contained in this paper are a first starting point before UAVs flight testing in a real situation around a frigate. They are a source of data obtained with wind tunnel scaled tests and can allow UAV designers to know the flow frequencies and turbulence intensity present on the flight deck of a frigate. The following step may be to use the same ultrasonic anemometers but placed on the flight deck of a real frigate. With all the data from the wind tunnel and the full-scale tests, the third phase of the tests can be carried out: flight-tests of UAV surrounding a frigate. The aircraft must be instrumented with pressure taps and accelerometers to record data during its flight around the frigate. Then, the complete process to be followed in order to understand the flow behind the frigate and its effect on UAVs flight is summarized in figure 4-1.

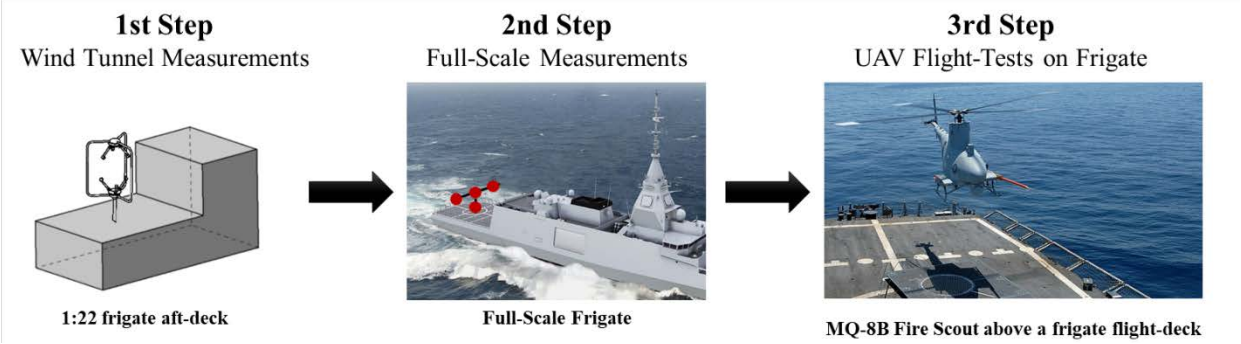

Figure 4-1: UAV flight test data acquisition process around frigates.

REFERENCES

[1] Dooley, G. M., Krebill, A. F., Martin, J. E., Buchholz, J. H. J., and Carrica, P. M., "Structure of a Ship Airwake at Multiple Scales," AIAA Journal, Vol. 58, No. 5, 2020, pp. 2005–2013. https://doi.org/10.2514/1.J058994

[2] Yuan, W., Wall, A., & Lee, R. (2018). "Combined numerical and experimental simulations of unsteady ship airwakes". Computers & Fluids, 172, 29-53.

[3] Crozon, C., Steijl, R., and Barakos, G. N., "Numerical Study of Helicopter Rotors in a Ship Airwake," Journal of Aircraft, Vol. 51, No. 6, 2014, pp. 1813–1832. https://doi.org/10.2514/1.C032535

[4] Forsythe, J., Lynch, E., Polsky, S., and Spalart, P., "Coupled Flight Simulator and CFD Calculations of Ship Airwake Using Kestrel," 53rd AIAA Aerospace Sciences Meeting, AIAA Paper 2015-0556, 2015. https://doi.org/10.2514/6.2015-0556

[5] Swales, C. and G. Breeze. 1997. "LDV measurements above the flight deck of a model frigate". In: 35th aerospace sciences meeting & exhibit, Reno, NV, 6-9. Reston, VA: AIAA.

[6] Brownell, C., L. Luznik, M. Snyder, H. Kang and C. Wilkinson. 2012. "In Situ Velocity Measurements in the Near-Wake of a Ship Superstructure". Journal of Aircraft. 49(5):1440-1450.

[7] Doane, S. R. and D.A. Landman. 2012. "A wind tunnel investigation of ship airwake/rotor downwash coupling using design of experiments methologies". In: Proceedings of the 50th AIAA Aerospace Sciences Meeting including the New Horizons Forum and Aerospace Exposition. 2012-0767.

[8] Bardera-Mora, R., Barcala-Montejano, M., Rodríguez-Sevillano, A., de Diego, G., & de Sotto, M. (2015). "A spectral analysis of laser Doppler anemometry turbulent flow measurements in a ship air wake". Proceedings Of The Institution Of Mechanical Engineers, Part G: Journal Of Aerospace Engineering, 229(12), 2309-2320.

[9] Wakefield, N. H., Newman, S. J., and Wilson, P. A., "Helicopter Flight Around a Ship's Superstructure," Proceedings of the Institution of Mechanical Engineers, Part G: Journal of Aerospace Engineering, Vol. 216, No. 1, 2002, pp. 13–28. https://doi.org/10.1243/0954410021533391

[10] Thedin, R., Kinzel, M. P., Horn, J. F., and Schmitz, S., "Coupled Simulations of Atmospheric Turbulence-Modified Ship Airwakes and Helicopter Flight Dynamics," Journal of Aircraft, Vol. 56, No. 2, 2019, pp. 812–824. https://doi.org/10.2514/1.C035158

[11] Thedin, R., Murman, S., Horn, J., and Schmitz, S., "Effects of Atmospheric Turbulence Unsteadiness on Ship Airwakes and Helicopter Dynamics," Journal of Aircraft, Vol. 57, No. 3, 2020, pp. 534–546. https://doi.org/10.2514/1.C035643

[12] Van Muijden, J., Boelens, O., van der Vorst, J., and Gooden, J., "Computational Ship Airwake Determination to Support Helicopter-Ship Dynamic Interface Assessment," 21st AIAA Computational Fluid Dynamics Conference, AIAA Paper 2013-3078, 2013. https://doi.org/10.2514/6.2013-3078

[13] Kääriä, C. H.,Wang, Y., White, M. D., and Owen, I., "An Experimental Technique for Evaluating the Aerodynamic Impact of Ship Superstructures on Helicopter Operations," Ocean Engineering, Vol. 61, March 2013, pp. 97–108. https://doi.org/10.1016/j.oceaneng.2012.12.052

[14] Lee, R. and S. Zan. 2005. "Wind Tunnel Testing of a Helicopter Fuselage and Rotor in a Ship Airwake". Journal of the American Helicopter Society. 50(4):326-337.

[15] Wadcock, A. J., G. K. Yamauchi, J. T. Heineck, M. J. Silva and K. R. Long. 2004. "PIV Measurements of the Wake of a Tandem-Rotor Helicopter in Proximity to a Ship". National Aeronautics and space administration moffett field CA AMES research center.

[16] Adrian, R., and Westerweel, J., Particle Image Velocimetry, Cambridge Univ. Press, Cambridge, England, U.K., 2001.

[17] Prasad, A. K., "Particle Image Velocimetry," Current Science-Bangalore, Vol. 79, No. 1, 2000, pp. 51–60.

[18] Adrian, R., "Particle-Imaging Techniques for Experimental Fluid-Mechanics," Annual Review of Fluid Mechanics, Vol. 23, No. 1, 1991, pp. 261–304. https://doi.org/10.1146/annurev.fl.23.010191.001401

[19] Raffel, M., Willert, C., Scarano, C., Wereley, S., and Kompenhans, J., Particle Image Velocimetry, Springer, Germany, 2007.

[20] WindMaster (Part 1590-PK-020) & WindMaster Pro (Part 1561-PK-020) Ultrasonic Anemometer User Manual Doc No. 1561-PS-0001 Issue 03

[21] Harrison, S., Wall, A. Thornhill, E. "Assessing Pilot response to Low-Frequency Disturbances: A Literature Review." CASI AERO 2019.